Ab Initio Molecular Orbital Study on the Electronic Structures and Reactivity of Boron-Substituted Carbon

Xianxian Wu* and Ljubisa R. Radovic

Department of Energy and Geo-Environmental Engineering, The Pennsylvania State University, University Park, Pennsylvania 16802

Received: April 23, 2004; In Final Form: June 18, 2004

A study using ab initio MO calculations and frontier orbital theory has been performed to investigate the effect of substitutional boron on the electronic structure and reactivity of eight-ring carbon model structures. This theoretical analysis confirmed that boron substitution in the carbon lattice can result in two opposite effects on carbon oxidation: catalysis and inhibition. Boron substitution was found to decrease the global cluster stability and to affect the local reactivity of its edge sites. For a zigzag cluster, the reactivity of carbon active sites may be increased or decreased by boron substitution and the exact effect appears to be dependent on substituent position: in general, the reactivity of unsaturated edge sites decreases, but substitution at certain basal-plane sites may increase the reactivity of some active sites which in turn suggests a catalytic effect. For an armchair cluster, boron substitution increases the reactivity of one or more armchair edge sites. Single atom substitution in the zigzag cluster may result in thermodynamically favorable or unfavorable O_2 chemisorption; the exact effect was found to be site-dependent. It also increases the energy barrier for CO desorption. Such an intriguing dual effect provides an explanation for the experimentally observed conflicting effects of boron doping in carbon oxidation.

1. Introduction

Boron is by far the most widely used doping element in carbon.[1] It is the only atom that enters the graphite lattice by substituting for carbon at the trigonal sites and consequently alters the electronic properties of the material.[2−4] Boron has been used to dope graphite,[2,5−8] carbon/carbon composites,[9−11] and other carbon materials[12−20] to improve their oxidation resistance. Boron substitution has also been applied to improve carbon's capacity as anode material in Li ion batteries.[21−27] Recently, boron also has been introduced into carbon nanotubes[28−34] as well as diamond electrodes[35−37] to change their electronic properties and electrochemical behavior. The unique ability of situating boron in the bulk of the material's structure means that it can be exploited for improving the oxidation resistance of friction materials, such as C/C composites used for aircraft brakes. Unlike dopants such as phosphorus,[38] the inhibiting effect of boron is not jeopardized by surface loss due to friction.

These practical applications have resulted in the need to achieve better quantitative understanding of the effects of substitutional boron on the properties of doped carbon materials and the relevant mechanisms. Because boron has one electron less than carbon and an empty p orbital, and is thus expected to change the electron acceptor level, a straightforward explanation in terms of lower Fermi level of the doped carbons has been invoked to account for the modified electronic and physicochemical properties.[1,13,31] However, such an explanation has been found insufficient for understanding the modification of carbon reactivity.[15] Especially, the enhancement of oxidation resistance at relatively high levels of boron doping and a catalytic effect at low levels of boron doping[5,14] require a theoretical explanation.

Several theoretical explorations based on semiempirical molecular orbital (MO) calculations have already been conducted in attempts to elucidate the effect of substitutional boron on carbon's electronic properties.[15,39,40] Boron substitution might change the density distribution of high energy electrons along the edges of carbon layer and consequently reduce the total number of active sites.[39] Such a electron density reduction might result in a suppression of O_2 chemisorption.[15] Although those studies provided interesting arguments on the dual effect of substitutional boron on the reactivity of carbon, some fundamental issues still need to be further clarified.[15] There is, then, a need to reevaluate the electronic effect of boron-substitution by using the advanced method such as ab initio calculations. The usefulness of this tool in furthering the understanding of carbon reactivity has been demonstrated by Yang's group[41−43] and extended by other investigators.[44−54]

In the present study, we studied the effect of substitutional boron on the electronic structures and reactivity of two 8-ring model carbon structures using ab initio method. Fukui's frontier orbital theory[55,56] was used to explore a relationship that the highest occupied molecular orbital (HOMO) and the lowest unoccupied molecular orbital (LUMO) may have with the behavior of carbon in oxidation reactions. Besides using these global properties as indicators of kinetic stability, an evaluation of local reactivity of each edge site in the cluster with respect to electrophilic attack was conducted. The enthalpy changes of O_2 chemisorption on the (re)active sites and the decomposition of a surface complex to form CO were also studied.

2. Computational Details

The commercial Gaussian 98 software package[57] was used in all calculations. The selected model structures ($C_{28}H_{10}$) are shown in Figure 1: the zigzag cluster A has four free (unsaturated) zigzag edge sites and the armchair cluster B has

* To whom correspondence should be addressed. E-mail: x3w@ornl.gov.

10.1021/jp048212w CCC: $27.50
Published on Web 09/18/2004

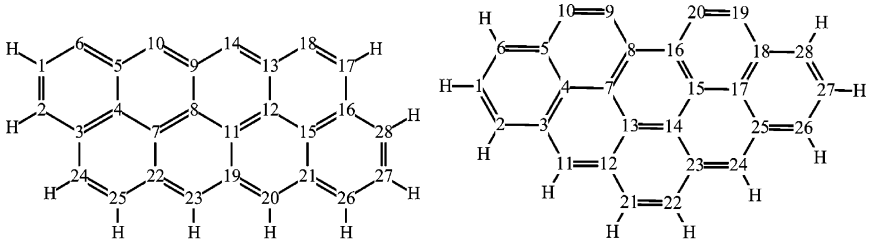

Model Cluster A **Model Cluster B**

Figure 1. Selected model structures for molecular orbital calculations.

four free armchair edge sites; all other edge sites are terminated with hydrogen atoms. Up to four substituted boron atoms were considered for electronic structure calculations in the presence of substitutional boron. Based on reports that O_2 attack on carbons is often dominated by the oxidation of zigzag sites,[58−60] cluster A was selected to evaluate the effect of boron on O_2 chemisorption and CO desorption. Single atom substitution at an edge or basal-plane site was examined in some detail.

The model chemistry selected for the calculations is HF/6-31G(d)//B3LYP/6-31G(d) which was used in previous work.[49] The HF/6-31G(d) method was employed for geometry optimization and frequency calculations, whereas B3LYP/6-31G(d) was used for calculating the self-consistent field (SCF) energies and bond populations.[41] The choice of spin multiplicity for each calculation, especially for boron-containing clusters, was not analyzed in detail but was determined here using the method suggested by Kyotani and Tomita:[44] the values selected were the ones that resulted in reasonable chemical structures, with minimum spin contamination and the lowest energy state. For the open-shell systems, the B3LYP density functionals should be developed only in the spin-unrestricted formalism.[61] There are small differences between unrestricted and restricted open-shell wave functions, and the B3LYP method suffers from much smaller spin contamination than HF.[46] The population analysis in this study is based, therefore, on the unrestricted open-shell method.

The enthalpy of adsorption (ΔH_{ads}) was determined in the standard fashion

$$\Delta H_{ads} = H_{graphene-oxygen} - H_{graphene} - 2H_{O_2}$$

Here $H_{graphene-oxygen}$ is the enthalpy of the optimized model structure with four chemisorbed oxygen atoms at the edge sites, $H_{graphene}$ is the enthalpy of the corresponding optimized model structure, and H_{O_2} is the enthalpy of O_2.

The bond dissociation energy for CO desorption was calculated using standard procedures (scan mode in Gaussian 98). Briefly, after geometry optimization, single-point energy (SPE) was calculated upon each equilateral change of the lengths of the two C−C bonds adjacent to the C═O moeity. When there was no additional change in the total energy upon further bond length increase, the difference between the total constant energy and the lowest SPE was taken as the bond energy.

3. Results and Discussion

3.1. Effects of Substitutional Boron on Electronic Structure and Reactivity. The optimized geometries of model structures A and B and their boron-substituted counterparts confirm that all clusters remain 2-dimensional graphene sheets because all dihedral angles are very close to 0.0 or 180.0°. The average bond lengths are 1.42 Å in cluster A and 1.40 Å in cluster B. The average C−C−C bond angles are very close to 120.0° for both structures. In agreement with recent results of Endo et al.,[23] boron substitution is seen to increase the bond lengths. As shown in Figure 2 using boron substitution at position #12 in cluster A, the three bonds of the boron atom all become ca. 0.1 Å longer.

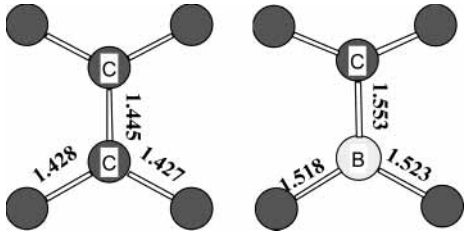

Figure 2. Effect of boron substitution at position #12 in model cluster A on calculated bond lengths. (The units shown are Å.).

TABLE 1: Calculated Orbital Energies for HOMO and LUMO, HOMO−LUMO Gaps, and Hardness η for Model Clusters A and B with One Substituted Boron Atom

position of boron substitution	HOMO (eV)	LUMO (eV)	LUMO−HOMO (eV)	η (eV)
model A	−4.957	−2.648	2.309	1.155
#9	−4.962	−2.773	2.189	1.095
#10	−4.400	−2.448	1.952	0.976
#11	−4.897	−3.021	1.876	0.938
#12	−4.954	−2.823	2.131	1.066
#19	−4.970	−2.816	2.154	1.077
#23	−4.853	−2.487	2.366	1.183
model B	−5.128	−2.261	2.867	1.434
#15	−5.058	−2.780	2.278	1.139
#16	−5.030	−2.605	2.425	1.213

Table 1 lists the orbital energies, LUMO−HOMO energy gap, and the hardness of single boron atom substituted clusters A and B. Oxidation is assumed to be an electrophilic reaction in which oxygen draws electrons from the carbon. Therefore, the propensity of carbon to donate its electrons can be taken as an index of its reactivity. It is further assumed that the oxidation potential is related to the ionization potential,[62] and the latter corresponds to the negative value of the highest occupied DFT orbital energy.[63] (The HOMO energy then gives the first ionization potential of the molecule and the LUMO energy is a measure of the first electron affinity.) A higher HOMO energy of the cluster is thus interpreted as a higher oxidation reactivity. Furthermore, according to Pearson's maximum hardness principle,[64,65] increased stability is obtained by increased hardness of a molecule at equal electronegativity and equal external potential. The absolute hardness η is calculated from the energy gap, as $\eta = (\epsilon_{LUMO} - \epsilon_{HOMO})/2$, where ϵ_{HOMO} and ϵ_{LUMO} are the energies of the frontier orbitals. A large energy gap implies high kinetic stability and low chemical reactivity,[66] because it is energetically unfavorable to add electrons to a high-lying LUMO, to extract electrons from a low-lying HOMO, and thus form the activated complex in any potential reaction.

TABLE 2: Calculated Orbital Energies for HOMO and LUMO, HOMO−LUMO Gap and Hardness η for Model Clusters A and B with More than One Substituted Boron Atom

position of boron substitution	HOMO (eV)	LUMO (eV)	LUMO−HOMO (eV)	η (eV)
model A				
#9+#10	−4.596	−2.448	2.148	1.074
#10+#18	−4.283	−2.364	1.918	0.959
#6+#18	−4.246	−2.197	2.049	1.024
#19+#23	−4.718	−3.899	0.819	0.409
#20+#23	−4.994	−4.385	0.609	0.304
#6+#10+#14+#18	−3.984	−2.360	1.624	0.812
model B				
#19+#20	−4.511	−3.552	0.959	0.480
#9+#10+#19+#20	−4.115	−3.701	0.414	0.207

As shown in Table 1, a very slight change is seen for the HOMO of cluster A upon single boron atom substitution, except for substitution at edge site #10 which shifts the energy upward by ca. 0.5 eV. Substitution at #9 or #19 is seen to decrease HOMO to some extent, whereas substitution at #11, #12, or #23 has the opposite effect. From the HOMO energy values it is concluded that boron substitution in a zigzag cluster may result in either inhibiting or catalytic effect, depending on the substituent position. Substitution at an edge (unsaturated) site lowers the oxidation potential and this can be interpreted as facilitating oxidation. This result is opposite to that of semiempirical MO calculations,[39] in which boron substitution at the edge sites was reported to cause a significant inhibition effect. In cluster B, boron substitution at #15 or #16 is also seen to increase the HOMO slightly, indicating that boron lowers its ionization potential and thus suggests a catalytic effect. In previous studies,[7,67,68] it has been proposed that boron blocks primarily the zigzag sites, while no armchair site inhibitors have been identified.[69] Our results offer an explanation for such observations: boron substitution does not result in the inhibition of oxidation of the armchair sites, although it may result in such an effect on the zigzag sites.

Boron substitution is seen to decrease the LUMO for clusters A and B except at #10 or #23 of cluster A. The lowering of LUMO has been proposed as a main reason for the large Li storage capacity in boron-doped disordered carbons.[40] These exceptions to the general trends in both HOMO and LUMO energies noted for edge atom substitution (at unsaturated edge site #10 or at H-saturated edge site #23) suggest that substitution at edge sites results in a larger change in both electron donation and acceptance capacity of the graphene sheet than substitution at basal-plane positions.

The HOMO−LUMO energy gap or hardness reveals an additional trend in boron substitution. Generally, the gap is associated with chemical stability against electronic excitation. The hardness values shown in Table 1 indicate that boron substitution in general reduces the HOMO−LUMO gap, or makes both clusters softer, with substitution at #23 as the only exception. So, based on this global property, it can be concluded that boron substitution generally reduces the stability of carbon and makes it more susceptible to O_2 attack.

The effects of multiple boron atom substitution on the same global properties are summarized in Table 2. Substitution at two sites also results in a lower oxidation potential and lower hardness of both clusters. When boron replaces all four edge sites, more than 1.0 eV increase is seen for the HOMO energy, accompanied by a hardness decrease. The changes in these properties suggest a significant destabilizing effect of edge substitution and reinforce the expectation of a catalytic effect.

TABLE 3: Effect of Boron Substitution on the Total Spin Density at Four Edge Sites in Model Cluster A

position of boron substitution	edge site			
	6	10	14	18
model A	1.196	1.315	1.273	1.138
#9	1.189	1.336	−1.107	0.893
#10	1.127	0.283	1.201	1.122
#11	1.146	1.222	−0.684	1.004
#12	1.105	1.136	−0.731	0.857
#19	1.224	1.270	−0.819	0.976
#23	1.293	1.353	−0.849	1.016

Similar results have also been obtained in a semiempirical AM1 quantum chemistry calculation:[70] boron substitution lowers LUMO, raises HOMO and thus decreases the energy gap.

It is well-known that the vacancies and edge atoms on the carbon surface are the (re)active sites and only these sites contribute directly to the gasification reactions,[59,60] whereas the basal-plane sites do not participate directly in oxygen chemisorption and formation of gaseous products.[71] These considerations make a local reactivity study of carbon sites both interesting and desirable. In addition, the HOMO and LUMO energy levels of O_2 are −5.767 and −3.804 eV (so its hardness is 0.982 eV). The gap between the frontier orbitals of the reactants (a specified cluster and O_2) is small, and the reacting system is soft. The rate and the direction of the reaction are then orbital-controlled.[63] So it is necessary to analyze also the cluster's local properties to achieve a better understanding of its reactivity.

In agreement with the results for a seven-ring zigzag model structure,[49] analysis of the spin density of cluster A shows that the unpaired electrons are mainly located on the zigzag edge sites 6, 10, 14, and 18. Table 3 summarizes the results obtained using the Mulliken population analysis. Because open-shell calculation was used, it is normal to get negative numbers for the spin density values at some sites.[72] In the presence of boron, the unpaired electron density remains on the edge sites, although boron substitution affects the density on each site. In addition, relatively larger changes occur at sites 14 and 18 than at sites 10 and 6. The #10 substitution is seen to reduce the spin density at site #10 only, with very slight influences on other edge sites.

More detailed electron population analyses show that the HOMOs in these open-shell systems mainly consist of $2p_z$ and $3p_z$ orbitals of carbon atoms with very slight contribution from 4*xz* and 4*yz* orbitals. All of the coefficients for other atomic orbitals are essentially zero. This indicates the formation of π MOs perpendicular to the $x-y$ plane, as expected. Typical electron density contours of the HOMOs for boron-substituted cluster A are shown in Figure 3, and those for cluster B are shown in Figure 4. An analysis of these contours shows that boron substitution in either the zigzag or armchair cluster causes a redistribution in the HOMO electron density: a prominent part of the electron density is centered on the four unsaturated zigzag edge sites without bonding to the adjacent atoms, whereas there is no significant electron density located around the four armchair edge sites (sites 9, 10, 19, and 20 in cluster B of Figure 1). Because in a reaction with an electrophilic agent the most susceptible site to attack is that position of the substrate at which the HOMO electron density is the highest,[55,56] the difference between the HOMO electronic structures of the zigzag and armchair sites is taken as an explanation for the often observed difference in the reactivities of these edge sites: zigzag sites have been reported to be more reactive than armchair sites.[73,74] A more detailed study of this difference and its effect on the chemisorption and desorption steps in carbon oxidation has been

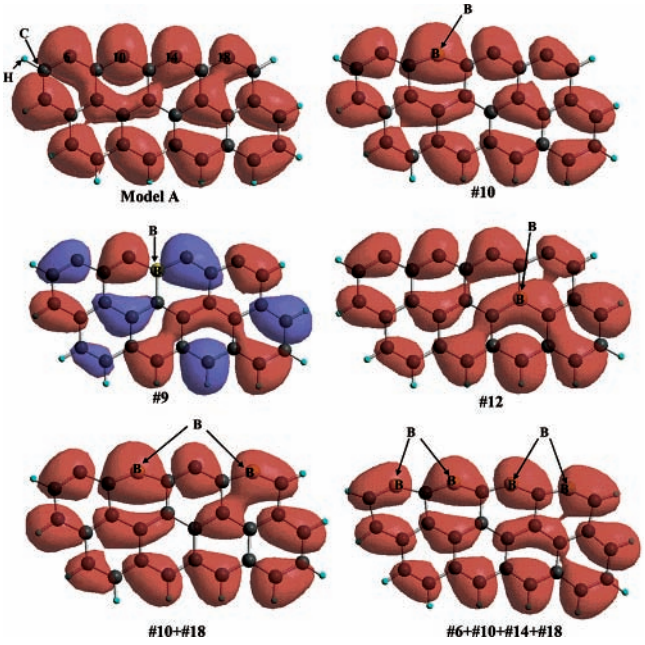

Figure 3. HOMO for boron-substituted zigzag model cluster A.

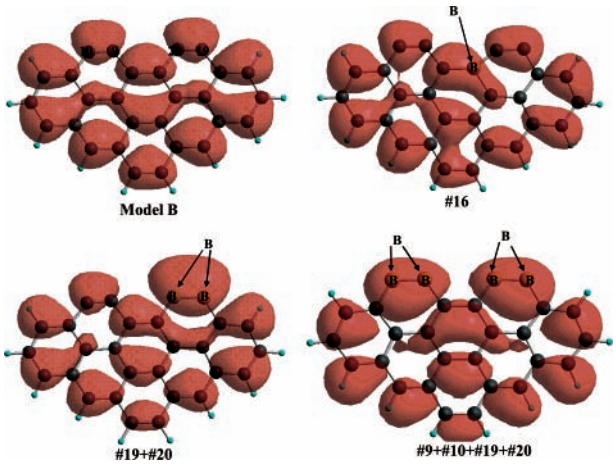

Figure 4. HOMO for boron-substituted armchair model cluster B.

conducted in a complementary study by our group.[49] Here we will focus on the effects of boron substitution. With substitutional boron located at the edge sites, a significant reduction in the density of high energy electrons on these sites, predicted by semiempirical (MOPAC) calculation[39] is not clearly observed here. Instead, the electron density on these sites (e.g., site 10, or sites 10 and 18 in Figure 3) seems to increase. This effect becomes pronounced in the armchair cluster: edge site substitution clearly increases the HOMO electron density on these sites (Figure 4). The above observations on the orbital contours confirm that boron substitution indeed changes the reactivity of carbon edge sites.

In what follows, the local HOMO electron density is used as an approximation to the Fukui indices, and we further discuss the influence of boron substitution based on these quantitative results. In the Gaussian 98 program, the molecular orbitals are expanded in terms of a set of N basis functions, ϕ_μ, and the electron density function $\rho(r)$ is given as[75] $\rho(r) = \sum_\mu^N \sum_\nu^N P_{\mu\nu}\phi_\mu\phi_\nu$, where $P_{\mu\nu} = \sum_i C_{i\mu} C_{i\nu}$, and $C_{i\mu}$ is the coefficient of μth atomic orbital in the ith molecular orbital. The calculated local HOMO electron densities for the four edge sites in cluster A and the effect of boron substitution at different positions on their densities as well as the density of boron site(s) (if not at the edge) are listed in Table 4. For comparison, the densities at additional two sites with the highest value (except the edge sites) are shown as well. Similarly, the HOMO electron densities at the edge sites in cluster B and their changes upon boron substitution are shown in Table 5.

As shown in Table 4, the electron density at the four zigzag edge sites is in general reduced by boron substitution. In cluster A, site 10 has the highest density, followed by sites 2, 14 and 6. Boron substitution at #10 or #19, or at 10 and 18, results in a slight density decrease at 10, but this site still has the highest density. Substitution at 9 or 12 or at all four edge positions turns sites 20 and 28 into the highest density sites and significantly reduces the density at the four edge sites. When substitution occurs at a relatively distant position from the edge (e.g., 11 or 23), the density at two of the edge sites increases and at the other two it decreases: substitution at 11 increases the density at sites 14 (the highest one) and 18, and substitution at 23 increases the density at sites 6 and 10 (the highest one). The above observations suggest that the effect of substitution on the local reactivity of each carbon site is quite sensitive to boron location and that the site having the highest density (the highest local reactivity) always is the edge carbon atom (either unsaturated or H-saturated site). In carbon oxidation, these unsaturated edge sites are of greatest interest, and below we discuss their local reactivity in greater detail.

Again, the density values at edge sites are also small in cluster B, which indicates the low reactivity of these sites. Boron substitution at basal-plane sites (e.g., #15 or #16) only causes a slight electron density increase at the far edge site (#10) from the substitution position and a decrease at other three edge sites. As illustrated in Figure 4 and listed in Table 5, however, when boron atoms substitute for edge carbon in a pair, the densities at these edge sites are significantly increased. For example, substitution at 19 and 20 causes that over 20% of the total electron density in the HOMO becomes concentrated on these two edge sites. Therefore, these two sites have the highest reactivity.

Fukui[55,56] has explained the behavior of naphthalene in electrophilic reactions within the framework of the frontier orbitals. According to this concept, a position with a higher frontier electron density has a higher reactivity toward electrophilic attack. Fukui showed that the difference between electron densities in the HOMO of a naphthalene molecule is sufficiently high for preferential electrophilic attack almost exclusively at the α position. This concept has also been successfully used for explaining the reactivity of other organic molecules,[63] for interpreting the shape-selective isopropylation of naphthalene over mordenite catalysts,[76] and for predicting reactivity in sterically complex systems.[77] Oskouie et al.,[78] as well as Tamon and co-workers,[79] have attempted to use this concept to explain adsorbate−adsorbent interaction in aqueous phase adsorption process. Ma et al.[39] also used it to calculate a reactivity index from the electron density in four highest occupied MOs. In what follows, we use the same approach to explore the effects of boron substitution.

If we start with the absolute values of electron density on the edge sites, boron substitution in cluster A was generally shown to reduce their local reactivity which in turn implies an inhibiting effect on O_2 chemisorption.[15] An exception to this general trend is the substitution at basal-plane sites far from free edge sites (e.g., at #11 or #23) in which the opposite effect is seen at two of the four edge sites. In contrast, boron substitution in cluster B shows a different trend: edge site substitution results in a catalytic effect, whereas basal-plane

TABLE 4: Calculated HOMO Electron Densities at Four Zigzag Edge Sites and Other High Density Sites of Model Cluster A

position of boron substitution	edge site 6	10	14	18	boron site	sites with the highest ρ[a]	
model A	0.107	0.176	0.115	0.026		0.119 (2)	0.044 (20)
#9	0.034	0.070	0.055	0.016	0.000	0.162 (20)	0.112 (28)
#10	0.083	0.160	0.098	0.021		0.092 (2)	0.062 (20)
#11	0.016	0.078	0.203	0.036	0.047	0.066 (12)	0.068 (20)
#12	0.030	0.057	0.045	0.009	0.020	0.244 (20)	0.117 (28)
#19	0.084	0.139	0.076	0.015	0.018	0.122 (20)	0.095 (2)
#23	0.129	0.195	0.063	0.014	0.024	0.143 (2)	0.062 (24)
#10 + #18	0.073	0.145	0.100	0.034		0.083 (2)	0.053 (20)
4 edge sites	0.022	0.044	0.045	0.021		0.118 (20)	0.108 (28)

[a] Excluding the 4 unsaturated edge sites.

TABLE 5: Calculated HOMO Electron Densities at Four Armchair Edge Sites and Other High Density Sites of Model Cluster B

position of boron substitution	edge site 9	10	19	20	boron sites	sites with the highest ρ[a]	
model B	0.018	0.032	0.032	0.018		0.089 (11)	0.089 (24)
#15	0.0002	0.041	0.001	0.001	0.027	0.148 (24)	0.103 (11)
#16	0.005	0.065	0.034	0.017	0.021	0.147 (11)	0.115 (6)
#19+#20	0.006	0.031	0.116	0.101		0.081 (28)	0.079 (26)
4 armchair sites	0.052	0.086	0.086	0.052		0.069 (6,28)	0.066 (2,26)

[a] Excluding the 4 unsaturated edge sites.

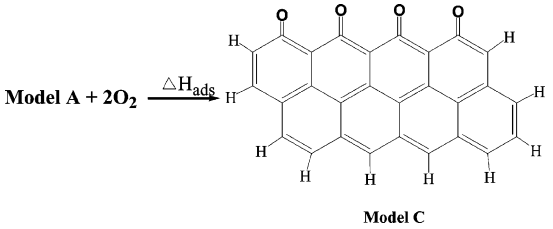

Figure 5. Representation of oxygen chemisorption for model cluster A.

substitution increases the reactivity of some edge sites and decreases that of others. A previous semiempirical MO study[15] showed that boron substitution results in a general π electron density decrease at the edge carbon atoms, but an increase in some sites, especially when boron is located at an armchair site, was also noted. This increase was found to be more pronounced for larger clusters. Using a 54-atom cluster, Ma et al.[39] reported similar large variations in electron densities of the edge sites due to boron substitution.

Clearly, both previous studies and the results presented here suggest the structure sensitivity of boron substitution; the net effect appears to depend on the type of edge site and the substituent location. In an attempt to further clarify the role of substitutional boron in carbon oxidation, separate calculations on the chemisorption of O_2 and desorption of CO were carried out and their results are presented in the following sections.

3.2. Effect of Substitutional Boron on O_2 Chemisorption. The purpose of doing the chemisorption calculation was to see if there is a uniform (thermodynamic) trend upon introduction of substitutional boron. As shown in Figure 5, cluster C represents a graphene structure containing four oxygen atoms chemisorbed on the edge sites of cluster A. The calculated adsorption energies (ΔH_{ads}) are listed in Table 6. The same calculations have been done for the boron-substituted cluster A. The corresponding values of the total energy of the boron-substituted cluster before O_2 chemisorption and the adsorption energy are also given in Table 6. An examination of the geometry of the clusters whose edge sites are saturated with carbonyl oxygen confirms that they remain planar. The C−O bond lengths in cluster C and its boron-substituted counterparts

TABLE 6: Effect of Substitutional Boron on the Adsorption Heat (at 298 K) of O_2 and the Lengths of C−O Bonds in Model Cluster A

position of boron substitution	total energy (hartrees)	ΔH_{ads} (kJ/mol O_2)	C−O bond length (Å) at edge sites 6	10	14	18
model A	−1072.75443	−749.61	1.20	1.20	1.19	1.21
#9	−1059.49519	−803.47	1.24	1.32	1.32	1.24
#10	−1059.52347	−690.26	1.25	1.35[a]	1.34	1.35
#12	−1059.49369	−739.82	1.24	1.22	1.32	1.33
#19	−1059.47712	−787.24	1.23	1.34	1.34	1.24

[a] B−O bond.

are shown in Table 6: boron substitution results in the elongation of the C−O bonds. From this point of view, it seems that boron substitution weakens the C−O bond strength.

Boron substitution at positions #9, 10, 12, and 19 of cluster A is selected for chemisorption calculations because the electron densities of the four edges sites in the corresponding structures are all decreased as a consequence of boron substitution, and this reveals a decrease in adsorption affinity (kinetic implication). The adsorption energies (thermodynamic implication) in Table 6 do not give a uniform result regarding the influence of boron substitution; instead, it seems that this influence is site-dependent. Boron substitution at edge site #10 does make the chemisorption less thermodynamically favorable; but substitution at the basal-plane site #9 or #19 makes it favorable, and substitution at #12 only has a slight decreasing effect on the associated heat release. These site-sensitive dependences indicate that the attempt to correlate the effect of boron substitution on O_2 adsorption energy with its effect on the reactivities of carbon edge sites was not successful. A simulation study on carbon bond breakages, then was performed to evaluate its effect on the C−C bonds.

3.3. Effect of Substitutional Boron on CO Desorption. The desorption of a CO molecule from a zigzag edge site is represented in Figure 6. The energy curves (vs the elongation of bond length) for the C−C bond cleavage at site 14 are shown in Figure 7. The bond distance on the *x* axis is actually the distance from C(14) to the line between C(9) and C(13) along

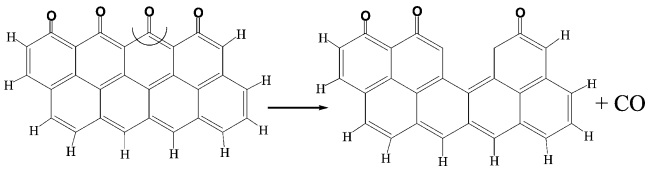

Figure 6. Representation of bond cleavage at an edge carbon atom in the presence of chemisorbed O.

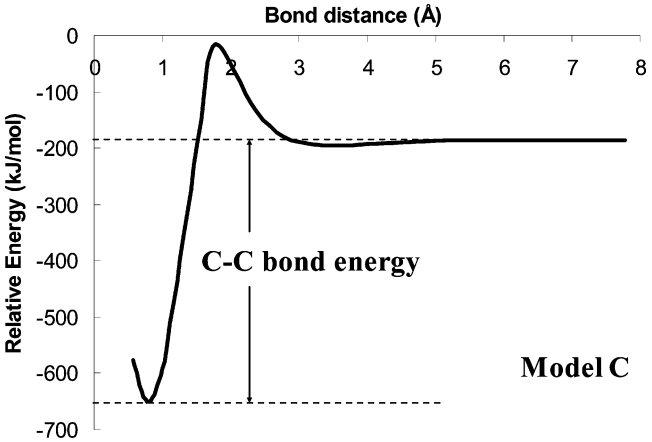

Figure 7. Energy vs C−C bond distance for model cluster C.

the direction of the O═C(14) bond (see Figure 1). The bond dissociation energy curves for the corresponding boron-substituted structures are shown in Figure 8. It should be noted that all of these curves in Figures 7 and 8 show a peak at around 2.0 Å. The possible reason for its appearance has been discussed by Montoya et al.[48] As shown in Figure 7 using the example of cluster C, here we use the difference between the lowest energy point and the dissociated bond energy on the curves as a measure of C−C bond energy. The results are listed in Table 7. As pointed out by Chen and Yang,[43] the calculated bond energy actually has units of kilojoules "per atom" which involves the cleavage of two C−C bonds; if their approach is used here, the

TABLE 7: Effect of Boron Substitution on Calculated Bond Energies (for the reaction represented in Figure 7)

position # of boron substitution	model C	#9	#10	#12	#19
bond energy (kJ/mol C)	463.5	490.7	547.4	640.4	621.2

calculated bond energy for CO desorption from unsubstituted cluster C is ca. 295.5 kJ/mol. This number is close to the experimental value of ca. 335.0 kJ/mol for graphite.[80] Because here we are only interested in relative effects of boron substitution, we shall analyze the numbers listed in Table 7.

From Table 7, the bond energy for CO desorption is seen to increase in the presence of substitutional boron either at the edge site or at the basal-plane site. This result suggests an inhibition effect of boron substitution on CO desorption. It is noteworthy that the boron contents represented by one or more than one atom substitution in the selected model structures are relatively high (single atom substitution results in 3.57% boron) due to the selected cluster size. If the liberation of CO from the active carbon−oxygen complexes (by breaking the neighboring C−C bonds) is considered as rate-limiting, the predicted inhibition effect by ab initio calculations here, then, could account for the experimentally observed inhibition effects at such high substitution level.[5,7,8,13,81] In addition, even though a catalytic effect was also observed when boron doping amount is relatively low (at the ppm level),[5,12,14] a direct prediction by ab initio calculations is not possible because of a computational limitation in cluster sizes that can be practically examined. A commonly used alternative approach is to analyze the electronic structure and predict the reactivity based on electronic parameters. In fact, a previous study[15] used simple Hückel and AM1 semiempirical MO calculations to anticipate the catalytic effect at low boron substitution level. The concept of π electron redistribution by boron substitution was suggested to account for the experimentally observed dual effect. The ab initio study here confirmed, to some extent, an inhibition effect is dominant at a high boron content but did not rule out the possibility of

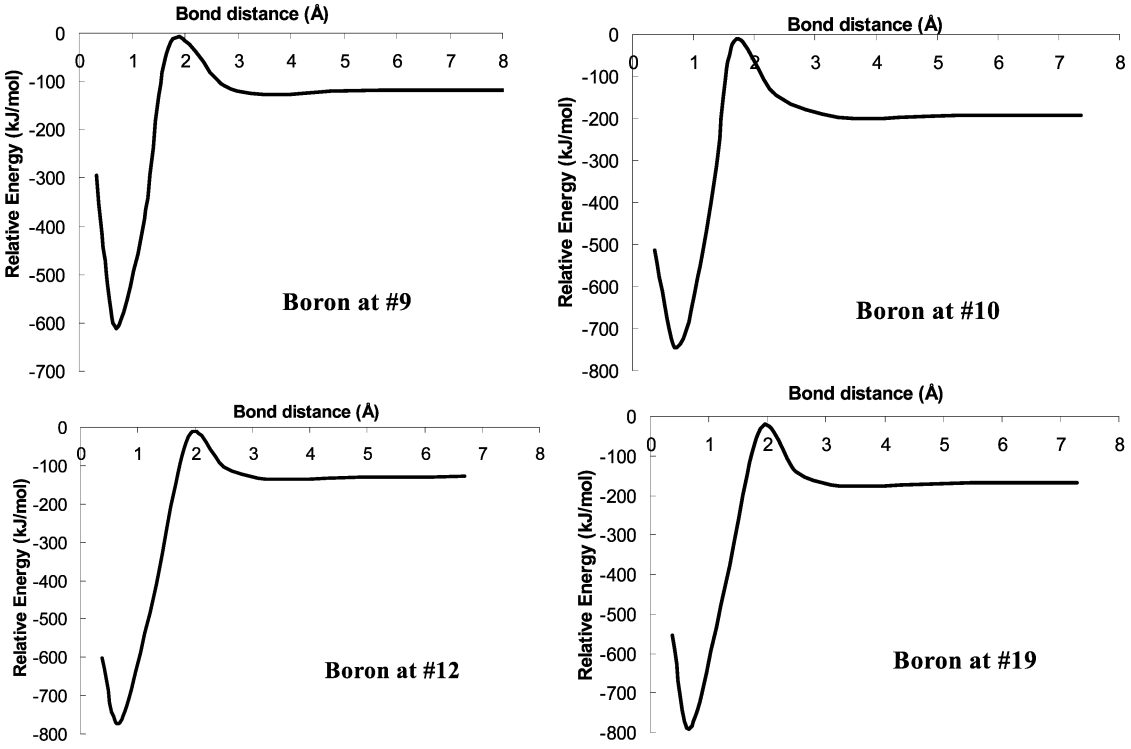

Figure 8. Energy vs C−C bond distance for boron-substituted model cluster C.

"catalytic effect" dominance at a low boron content. Furthermore, the consistency of the theoretical prediction with the experimental observations in this study also indicates the validity of using a finite polybenzenoid hydrocarbon to simulate an infinite graphene layer, as argued by Stein and Brown.[73]

4. Summary

Even though our theoretical approach shows promise in rationalizing some of the key experimental observations, its several limitations need to be acknowledged here. First, the eight-ring clusters are only about 10 Å wide and thus smaller than typical carbon crystallites (not to mention the 3-D structure in C/C composite materials). Second, limited by computational ability, the substitutional boron content cannot go down to a very low level (single atom substitution results in 3.57% boron). Third, boron substitution is known to have preferred locations (more disordered regions in the carbon structure); translating this knowledge into an effective theoretical criterion for substitution of edge vs basal-plane sites is not straightforward. Although more detailed ab initio studies are needed, this exploratory study does show clearly that boron substitution decreases the global stability of the model carbon clusters and modifies, in an apparently complex fashion, the local reactivity of the edge sites. The very intriguing effects extracted from theoretical explorations are interpreted as additional support for the experimentally observed dual effects of boron.

Acknowledgment. This study was made possible by the financial support from the Carbon Research Center at PSU.

References and Notes

(1) Marchand, A. Electronic properties of doped carbons. In *Chemistry and Physics of Carbon*; Walker, P. L., Jr., Ed.; Marcel Dekker: New York, 1971; p 155.
(2) Lowell, C. E. *J. Am. Ceram. Soc.* **1967**, *50*, 142.
(3) Marinkovic, S. Substitutional solid solubility in carbon and graphite. In *Chemistry and Physics of Carbon*; Thrower, P. A., Ed.; Marcel Dekker: New York, 1984; p 1.
(4) Serin, V.; Brydson, R.; Scott, A.; Kihn, Y.; Abidate, O.; Maquin, B.; Derrê, A. *Carbon* **2000**, *38*, 547.
(5) Allardice, D. J.; Walker, P. L., Jr. *Carbon* **1970**, *8*, 375.
(6) Hagio, T.; Nakamizo, M.; Kobayashi, K. *Carbon* **1989**, *27*, 259.
(7) Rodriguez, N. M.; Baker, R. T. K. *J. Mater. Res.* **1993**, *8*, 1886.
(8) Sogabe, T.; Matsuda, T.; Kuroda, K.; Hirohata, Y.; Hino, T.; Yamashina, T. *Carbon* **1995**, *33*, 1783.
(9) Ragan, S.; Emmerson, G. T. *Carbon* **1992**, *30*, 339.
(10) Kowbel, W.; Huang, Y.; Tsou, H. *Carbon* **1993**, *31*, 355.
(11) Wu, X.; Radovic, L. R. *Carbon* Submitted.
(12) Jones, L. E.; Thrower, P. A. *J. Chim. Phys.* **1987**, *84*, 1431.
(13) Jones, L. E.; Thrower, P. A. *Carbon* **1991**, *29*, 251.
(14) Zhong D. H.; Sano, H.; Uchiyama, Y.; Kobayashi, K. *Carbon* **2000**, *38*, 1199.
(15) Radovic, L. R.; Karra, M.; Skokova, K.; Thrower, P. A. *Carbon* **1998**, *36*, 1841.
(16) Cermignani, W.; Paulson, T. E.; Onneby, C.; Pantano, C. G. *Carbon* **1995**, *33*, 367.
(17) Cermignani, W. Synthesis, characterization and oxidation of boron-doped carbons. Ph.D. Thesis, The Pennsylvania State University, 1997.
(18) Durkic, T.; Peric, A.; Lausevic, M.; Dekanski, A.; Neskovic, O.; Veljkovic, M.; Lausevic, Z. *Carbon* **1997**, *35*, 1567.
(19) Jacques, S.; Guette, A.; Bourrat, X.; Langlais, F.; Guimon, C.; Labrugere, C. *Carbon* **1996**, *34*, 1135.
(20) Chesneau, M.; Beguin, F.; Conard, J.; Erre, R.; Thebault, J. *Carbon* **1992**, *30*, 714.
(21) Way, B. M.; Dahn, J. R. *J. Electrochem. Soc.* **1994**, *141*, 907.
(22) Flandrois, S.; Ottaviani, B.; Derre, A.; Tressaud, A. *J. Phys. Chem. Solids* **1996**, *57*, 741.
(23) Endo, M.; Kim, C.; Karaki, T.; Tamaki, T.; Nishimura, Y.; Matthews, M. J.; Brown, S. D. M.; Dresselhaus, M. S. *Phys. Rev. B* **1998**, *58*, 8991.
(24) Endo, M.; Kim, C.; Nishimura, K.; Fujino, T.; Miyashita, K. *Carbon* **2000**, *38*, 183.
(25) Tanaka, U.; Sogabe, T.; Sakagoshi, H.; Ito, M.; Tojo, T. *Carbon* **2001**, *39*, 931.
(26) Mukhopadhyay, I.; Hoshino, N.; Kawasaki, S.; Okino, F.; Hsu, W. K.; Touhara, H. *J. Electrochem. Soc.* **2002**, *149*, 39.
(27) Machnikowski, J.; Frackowiak, E.; Kierzek, K.; Waszak, D.; Benoit, R.; Beguin, F. *J. Phys. Chem. Solids* **2004**, *65*, 153.
(28) Wei, B. Q.; Spolenak, R.; Kohler-Redlich, P.; Ruhle, M.; Arzt, E. *Appl. Phys. Lett.* **1999**, *74*, 3149.
(29) Han, W. Q.; Bando, Y.; Kurashima, K.; Sato, T. *Chem. Phys. Lett.* **1999**, *299*, 368.
(30) Hsu, W. K.; Firth, S.; Redlich, P.; Terrones, M.; Terrones, H.; Zhu, Y. Q.; Grobert, N.; Schilder, A.; Clark, R. J. H.; Kroto, H. W.; Walton, D. R. M. *J. Mater. Chem.* **2000**, *10*, 1425.
(31) Kotosonov, A. S.; Shilo, D. V. *Mol. Mater.* **2000**, *13*, 113.
(32) Liu, K.; Avouris, P.; Martel, R., et al. *Phys. Rev. B* **2001**, *63*, Art. No. 161404.
(33) Watts, P. C. P.; Hsu, W. K.; Chen, G. Z., et al. *J. Mater. Chem.* **2001**, *11*, 2482.
(34) Gai, P. L.; Stephan, O.; McGuire, K.; Rao, A. M.; Dresselhaus, M. S.; Dresselhaus, G.; Colliex, C. *J. Mater. Chem.* **2004**, *14*, 669.
(35) Vinokur, N.; Miller, B.; Avyigal, Y.; Kalish, R. *J. Electrochem. Soc.* **1996**, *143*, 238.
(36) Goeting, C. H.; Jones, F.; Foord, J. S.; Eklund, J. C.; Marken, F.; Compton, R. G.; Chalker, P. R.; Johnston, C. *J. Electroanal. Chem.* **1998**, *442*, 207.
(37) Compton, R. G.; Foord, J. S.; Marken, F. *Electroanalysis* **2003**, *15*, 1349.
(38) Wu, X.; Radovic, L. R. *Carbon* Submitted.
(39) Ma, X. L.; Wang, Q.; Chen, L. Q.; Cermignani, W.; Schobert, H. H.; Pantano, C. G. *Carbon* **1997**, *35*, 1517.
(40) Kurita, N. *Carbon* **2000**, *38*, 65.
(41) Chen, N.; Yang, R. T. *Carbon* **1998**, *36*, 1061.
(42) Chen, S. G.; Yang, R. T. *Energy Fuels* **1997**, *11*, 421.
(43) Chen, N.; Yang, R. T. *J. Phys. Chem. A* **1998**, *102*, 6348.
(44) Kyotani, T.; Tomita, A. *J. Phys. Chem. B* **1999**, *103*, 3434.
(45) Montoya, A.; Truong, T. N.; Sarofim, A. F. *J. Phys. Chem. A* **2000**, *104*, 8409.
(46) Montoya, A.; Truong, T. N.; Sarofim, A. F. *J. Phys. Chem. A* **2000**, *104*, 6108.
(47) Montoya, A.; Truong, T.-T.; Mondragón, F.; Truong, T. N. *J. Phys. Chem. A* **2001**, *105*, 6757.
(48) Montoya, A.; Mondragón, F.; Truong, T. N. *J. Phys. Chem. A* **2002**, *106*, 4236.
(49) Zhu, Z. H.; Radovic, L. R.; Lu, G. Q.; Wu, X. "Computational chemistry of zigzag and armchair sites in carbon oxidation."; The international carbon conference, 2001, Lexington, USA.
(50) Radovic, L. R.; Bockrath, B. "On some key questions in the application of computational chemistry to carbon reactivity"; The international carbon conference, 2001, Lexington, USA.
(51) Yang, F. H.; Yang, R. T. *Carbon* **2002**, *40*, 437.
(52) Zhu, Z. H.; Lu, G. Q.; Finnerty, J.; Yang, R. T. *Carbon* **2003**, *41*, 635.
(53) Yang, F. H.; Yang, R. T. *Carbon* **2003**, *41*, 2149.
(54) Montoya, A.; Mondragon, F.; Truong, T. N. *Carbon* **2002**, *40*, 1863.
(55) Fukui, K.; Yonezawa, T.; Shingu, H. *J. Chem. Phys.* **1952**, *20*, 722.
(56) Fukui, K.; Yonezawa, T.; Nagata, C.; Shingu, H. *J. Chem. Phys.* **1954**, *22*, 1433.
(57) Frisch, M. J.; Trucks, G. W.; Schlegel, H. B.; Scuseria, G. E.; Robb, M. A.; Cheeseman, J. R.; Zakrzewski, V. G.; Montgomery, J. A., Jr.; Stratmann, R. E.; Burant, J. C.; Dapprich, S.; Millam, J. M.; Daniels, A. D.; Kudin, K. N.; Strain, M. C.; Farkas, O.; Tomasi, J.; Barone, V.; Cossi, M.; Cammi, R.; Mennucci, B.; Pomelli, C.; Adamo, C.; Clifford, S.; Ochterski, J.; Petersson, G. A.; Ayala, P. Y.; Cui, Q.; Morokuma, K.; Malick, D. K.; Rabuck, A. D.; Raghavachari, K.; Foresman, J. B.; Cioslowski, J.; Ortiz, J. V.; Stefanov, B. B.; Liu, G.; Liashenko, A.; Piskorz, P.; Komaromi, I.; Gomperts, R.; Martin, R. L.; Fox, D. J.; Keith, T.; Al-Laham, M. A.; Peng, C. Y.; Nanayakkara, A.; Gonzalez, C.; Challacombe, M.; Gill, P. M. W.; Johnson, B. G.; Chen, W.; Wong, M. W.; Andres, J. L.; Head-Gordon, M.; Replogle, E. S.; Pople, J. A. *Gaussian 98*, revision A.9; Gaussian, Inc.: Pittsburgh, PA, 1998.
(58) Hennig, G. R. Electron microscopy of reactivity changes near lattice defects in graphite. In *Chemistry and Physics of Carbon*; Walker, P. L., Jr., Ed.; Marcel Dekker: New York, 1966; p 1.
(59) Thomas, J. M. Microscopic study of graphite oxidation. In *Chemistry and Physics of Carbon*; Walker, P. L., Jr., Ed.; Dekker: New York, 1965; p 121.
(60) Yang, R. T. Etch-decoration electron microscopy studies of the gas-carbon reactions. In *Chemistry and Physics of Carbon*; Walker, P. L., Jr., Ed.; Dekker: New York, 1984; p 163.
(61) Pople, J. A.; Gill, P. M. W.; Handy, N. C. *Int. J. Quantum Chem.* **1995**, *56*, 303.
(62) Casida, M. E. *Phys. Rev. B* **1999**, *59*, 4694.

(63) Traven, V. F. *Frontier Orbitals and Properties of Organic Molecules*; Ellis Horwood Limited: West Sussex, England, 1992.
(64) Pearson, R. G. *J. Chem. Educat.* **1987**, *64*, 561.
(65) Pearson, R. G. *Acc. Chem. Res.* **1993**, *26*, 250.
(66) Aihara, J. *J. Phys. Chem. A* **1999**, *103*, 7487.
(67) Oh, S. G.; Rodriguez, N. M. *J. Mater. Res.* **1993**, *8*, 2879.
(68) Park, C.; Baker, R. T. K. *J. Phys. Chem. B* **1999**, *103*, 2453.
(69) Hippo, E. J.; Murdie, N.; Kowbel, W. *Carbon* **1989**, *27*, 331.
(70) Strelko, V. V.; Kuts, V. S.; Thrower, P. A. *Carbon* **2000**, *38*, 1499.
(71) Laine, N. R.; Vastola, F. J.; Walker, P. L., Jr. *J. Phys. Chem.* **1963**, *67*, 2030.
(72) Foresman, J. B.; Frisch, Æ. *Exploring Chemistry with Electronic Structure Methods*, 2nd ed.; Gaussian, Inc.: Pittsburgh, 1996.
(73) Stein, S. E.; Brown, R. L. Pathways to graphite: properties of very large polybenzenoid hydrocarbons. In *Molecular Structure and Energetics*; Liebman, J., Greenberg, A., Eds.; VCH Publishers, Inc.: New York, 1987; Vol. 2, Chapter 2, p 37.
(74) Klein, D. J.; Bytautas, L. *J. Phys. Chem. A* **1999**, *103*, 5196.
(75) Hehre, W. J.; Radom, L.; Schleyer, P. v. R.; Pople, J. A. *Ab Initio Molecular Orbital Theory*; John Wiley & Sons: New York, 1986.
(76) Song, C. S.; Ma, X. L.; Schmitz, A. D.; Schobert, H. H. *Appl. Catal. A* **1999**, *182*, 175.
(77) Clark, L. A.; Ellis, D. E.; Snurr, R. Q. *J. Chem. Phys.* **2001**, *114*, 2580.
(78) Oskouie, A. K.; Miura, Y.; Furuya, E. G.; Noll, K. E. *Carbon* **2002**, *40*, 1199.
(79) Tamon, H.; Aburai, K.; Abe, M.; Okazaki, M. *J. Chem. Eng. Jpn.* **1995**, *28*, 823.
(80) Huttinger, K. J. *Carbon* **1990**, *28*, 453.
(81) Lee, Y. J.; Radovic, L. R. *Carbon* **2003**, *41*, 1987.